Hydrothermal Synthesis of Layered Double Hydroxides (LDHs) from Mixed MgO and Al_2O_3: LDH Formation Mechanism

Zhi Ping Xu and Guo Qing (Max) Lu*

Australian Research Council (ARC) Centre for Functional Nanomaterials, School of Engineering, The University of Queensland, Brisbane, QLD 4072, Australia

Received November 1, 2004. Revised Manuscript Received January 6, 2005

The formation of MgAl layered double hydroxide (LDH) from physically mixed MgO and Al_2O_3 oxides upon hydrothermal treatment has been extensively investigated, and a formation mechanism has been proposed. We observed that the formation of LDH from the oxide mixture occurs upon heating at 110 °C. In general, LDH is the major component while the minor phases are mainly determined by the initial pH of the oxide suspension as well as the MgO/Al_2O_3 ratio. The neutrality in the initial suspension results in a minor $Mg(OH)_2$ as the impure phase, while the alkalinity in the suspension keeps some MgO unreacted throughout the whole hydrothermal treatment. We suggest that MgO and Al_2O_3 be hydrated into $Mg(OH)_2$ and $Al(OH)_3$, respectively, in the initial stage for all samples. We further suggest that in the neutral condition $Mg(OH)_2$ be quickly dissociated to Mg^{2+} and OH^- which then deposit on the surface of $Al(OH)_3/Al_2O_3$ to form a MgAl pre-LDH material. $Al(OH)_4^-$, ionized from $Al(OH)_3$ in the basic solution, deposits on the surface of $Mg(OH)_2/MgO$ to result in a similar MgAl pre-LDH material. Such a pre-LDH material is then well crystallized upon continuous heating via the diffusion of metal ions in the solid lattice. Such a dissociation−deposition−diffusion mechanism via two pathways has been supported by the phase composition, morphological features of crystallites, and [Mg]/[Al] ratios on the crystallite surface, and presumably applied to the general formation of LDHs with various synthetic methods, such as coprecipitation, homogeneous preparation, and reconstruction.

Introduction

Layered double hydroxides (LDHs) have attracted increasing interest because of their potential applications in areas such as catalysis, separation, and medicine.[1−3] These hydroxides have a general formula of $M^{2+}_{1-x}M^{3+}_x(OH)_2A_x{\cdot}nH_2O$, where $M^{2+} = Mg^{2+}$, Zn^{2+}, Ni^{2+}, etc., $M^{3+} = Al^{3+}$, Fe^{3+}, Ga^{3+}, etc., and $A = {}^1/_2(CO_3^{2-})$, Cl^-, OH^-, etc. Structurally they consist of stacked brucite-like ($M^{2+}(OH)_2$) layers in which M^{2+} ions are partially substituted by M^{3+} ions. The substitute on the layers necessitates the incorporation of anions, such as CO_3^{2-}, Cl^-, and OH^-, between the interlayer to balance the resulting positive charge.[1−3]

Various LDH compounds can be synthesized with several preparation methods. In general, the most commonly used method is coprecipitation at various or constant pH, followed by aging at a certain temperature.[1−3] Homogeneous precipitation using urea as the base source usually leads to big LDH CO_3 crystallites that are well crystallized into hexagonal platy sheets.[1,4] Reconstruction from mixed oxide, e.g., MgAl oxide that is generated by calcining $MgAl-CO_3$ LDH at a mild temperature (e.g., 500 °C), takes advantage of LDH's "memory" effect to prepare LDHs intercalated with any desirable anion, such as various inorganic, organic, and biomedical anions.[1,5−7] Other methods have been reviewed recently.[1] Recently, a novel preparation method from physically mixed MgO and Al_2O_3 oxides to synthesize $3R_2$-polytype LDH[8] has been reported.[9] In this study, we systematically investigated the preparation of LDH by hydrothermally treating mixed MgO and Al_2O_3 in water and found that this method could be used to prepare micrometer-scale LDH particles with an anion other than CO_3^{2-} and the obtained LDH particles could be tailored in size and morphology.

Although LDHs exist in nature and can be readily synthesized in the laboratory, their formation mechanism is far from clear. To the best of our knowledge, there are three different points of view regarding the formation of LDHs. Braterman et al.[10,11] studied the titration behavior of Mg^{2+} and Al^{3+} against NaOH and found the precipitation takes place in two steps, which results in a poorly crystallized LDH material. They found that the subsequent aging converts it to a well-crystallized LDH. Eliseev et al.[12] studied the effect of thermostatic conditions on the LDH crystallization. They noted that the agglomerate formed at the first stage is

* To whom correspondence should be addressed. Phone: 61-7-33653885. Fax: 61-7-33656074. E-mail: maxlu@cheque.uq.edu.au.

(1) Braterman, P. S.; Xu, Z. P.; Yarberry, F. In *Handbook of Layered Materials*; Auerbach, S. M., Carrado, K. A., Dutta, P. K., Eds.; Marcel Dekker: New York, 2004; p 373.
(2) Rives, V., Ed. *Layered Double Hydroxides: Present and Future*; Nova Science Publishers: New York, 2001.
(3) Cavani, F.; Trifiro, F.; Vaccari, A. *Catal. Today* **1991**, *11*, 173.
(4) Cai, H.; Hillier, A. C.; Franklin, K. R.; Nunn, C. C.; Ward, M. D. *Science* **1994**, *266*, 1551.
(5) Nakayama, H.; Wada, N.; Tsuhako, M. *Int. J. Pharm.* **2004**, *269*, 469.
(6) Hibino, T.; Tsunashima, A. *Chem. Mater.* **1998**, *10*, 4055.
(7) Bontchev, R. P.; Liu, S.; Krumhansl, J. L.; Voigt, J.; Nenoff, T. M. *Chem. Mater.* **2003**, *15*, 3669.
(8) Bookin, A. S.; Drits, V. A. *Clays Clay Miner.* **1993**, *41*, 551.
(9) Newman, S. P.; Jones, W.; O'Connor, P.; Dtamires, D. N. *J. Mater. Chem.* **2002**, *12*, 153.
(10) Boclair, J. W.; Braterman, P. S. *Chem. Mater.* **1999**, *11*, 298.
(11) Boclair, J. W.; Braterman, P. S.; Jiang, J.; Lou, S.; Yarberry, F. *Chem. Mater.* **1999**, *11*, 303.

10.1021/cm048085g CCC: $30.25 © 2005 American Chemical Society
Published on Web 02/10/2005

Table 1. Sample Preparation Conditions

sample	species initial molar ratio	time[a] (days)	initial pH[b]	final pH	[Mg]/[Al] (XPS)[c]
MAO4A	$MgO:Al_2O_3 = 4:1$	5	7.0	10.1	4.120
MAO4B	$MgO:Al_2O_3 = 4:1$	10	7.0	9.9	1.643
MACl6	$MgO:Al_2O_3:NaCl = 6:1:2.3$	10	7.0	12.2	1.789
MACl4	$MgO:Al_2O_3:NaCl = 4:1:2.0$	10	7.0	11.9	1.225
MACl3	$MgO:Al_2O_3:NaCl = 3:1:2.2$	10	7.0	11.8	1.118
MACl2	$MgO:Al_2O_3:NaCl = 2:1:2.2$	10	7.0	11.5	1.122
MAHC4A	$MgO:Al_2O_3:NaHCO_3 = 4:1:2.4$	5	8.3	9.9	2.722
MAHC4B	$MgO:Al_2O_3:NaHCO_3 = 4:1:2.4$	10	8.3	9.7	1.383
MAHC6	$MgO:Al_2O_3:NaHCO_3 = 6:1:2.5$	10	8.3	9.8	1.078
MAC4	$MgO:Al_2O_3:Na_2CO_3 = 4:1:2.0$	10	11.5	11.8	0.140

[a] The temperature for hydrothermal treatment was 110 °C. [b] The initial pH is a theoretical value assuming water is pure and the oxide hydration does not occur but the sodium salt is fully dissolved. [c] The [Mg]/[Al] atomic ratio was deduced from the Mg 2p and Al 2p XPS data.

amorphous but then converted to a layered structure. They thought that the conversion of tetrahedral to octahedral Al is a sign of well-crystallized LDH formation. Sato et al.[13] investigated the reconstruction from calcined LDHs in Na_2CO_3 solution, and proposed a topotactical mechanism of LDH formation on the basis of their SEM observations. Stanimirova et al.[14,15] examined the reconstructed products from Mg_2Al oxide in the presence of Mg^{2+}, Zn^{2+}, Ni^{2+}, Co^{2+}, Cu^{2+}, and Mg_3Al oxide in water and stipulated a plausible dissolution−crystallization mechanism. McLaughlin et al.[16] found LDH formation in a mixed suspension of $Mg(OH)_2$ and aluminum hydroxycarbonate and observed LDH growth occurring directly on the surface of $Mg(OH)_2$, which was consistent with the dissolution−crystallization process. Apparently, these different models have all been based on their different observations under different experimental conditions, all reflecting the complexity of the LDH formation process. In this study, we analyzed in detail the structures and compositions in products formed from the physically mixed MgO and Al_2O_3 oxides upon hydrothermal treatment, and postulated a dissociation−deposition−diffusion mechanism for LDH formation, which in general explains well the LDH formation under various natural and synthetic conditions.

Experimental Section

Materials Preparation. MgO and Al_2O_3 were prepared by calcining $Mg(NO_3)_2 \cdot 6H_2O$ and $Al(OH)_3$ at 600 °C for 4 h in air, respectively. As-made MgO has a specific surface area of 8.3 m^2/g, a pore volume of 0.012 cm^3/g, and a pore diameter of 2−5 nm. Al_2O_3 is more porous, with a pore volume of 0.27 cm^3/g, a specific surface area of 121 m^2/g, and a pore diameter of 3−6 nm.

All samples (Table 1) were synthesized by a hydrothermal method. For example, MgAl−OH LDHs (MAO4A and MAO4B in Table 1) were made from 0.102 g of Al_2O_3 (~1.0 mmol Al_2O_3) and 0.162 g of MgO (~4.0 mmol) with a molar ratio of MgO to Al_2O_3 of 4 in an aqueous suspension. The oxides were placed in an autoclave (50 mL in volume) with 40 mL of deionized water and thoroughly shaken. The autoclave was then hydrothermally treated at 110 °C for 5 and 10 days, respectively. As-prepared product was collected after centrifugation and washed with deionized water two times, followed by drying at 80 °C overnight. As for MgAl−CO_3 LDH (samples MAHC*n* and MAC), $NaHCO_3$ (2.4−2.5 mmol of HCO_3^-) or Na_2CO_3 (2.0 mmol) was added, subject to the same hydrothermal treatment as for MgAl−OH LDH. In particular, sample MACH6 was made from an initial mixture of 6/1/2.5 $MgO/Al_2O_3/NaHCO_3$, with more MgO added. Similarly, MgAl−Cl LDHs were made with various ratios of MgO to Al_2O_3 with NaCl under the same conditions (Table 1). The final pH of all mother liquors was measured, as listed in Table 1. In comparison, the initial pH was estimated assuming the equilibrium of the acid−base reaction but with no other reactions taking place.

Materials Characterization. X-ray diffraction (XRD) patterns were collected on a powder X-ray diffractometer (Rigaku Miniflex with a variable slit width) with Cu Kα radiation ($\lambda = 0.15418$ nm) at a scanning rate of 2 deg/min from $2\theta = 5°$ to $2\theta = 70°$. Infrared spectra were collected using KBr disks on a Perkin-Elmer 2000 FTIR spectrometer after 40 scans within 4000−400 cm^{-1} at a resolution of 2 cm^{-1}. The electron microscopic images were obtained on a JEOL JSM-6400F field emission scanning electron microscope at an acceleration voltage of 10 kV. By dropping a droplet of the LDH-containing suspension and drying, the sample was mounted on a carbon film supported on a holder, followed by sputtering with platinum. The surface elements, e.g., Mg and Al in particular, were analyzed by XPS−energy dispersive spectrometry (EDS) on an AXIS Hsi-165-Ultra (Kratos Analytical) by using an Al Kα X-ray source at a constant analyzer pass energy of 20 eV. The atomic ratio of Mg and Al ([Mg]/[Al]) was calculated from the area ratio of the Mg 2p and Al 2p peaks with the correction for atomic sensitivity factors. The specific surface area, pore volume, and pore diameter of MgO and Al_2O_3 were determined by the Brunauer−Emmett−Teller (BET) method and Barret−Joyner−Hallenda (BJH) method, respectively, from the adsorption isotherms of N_2 at 77 K collected in a NOVA-1200 apparatus.

Results

Formation of MgAl−OH LDH. As shown in Figure 1, the target phase MgAl−OH LDH has been identified with XRD patterns. The diffraction peaks at low angles, as indexed with (003) and (006) for a rhombohedral symmetry (3R),[3] are very pronounced in sample MAO4B, which was obtained after 10 days of hydrothermal treatment. The interlayer spacing (0.752−0.756 nm) is in good agreement with that reported for MgAl−OH LDH.[17] We note that there are many other accompanied diffraction peaks, such as (012), (014), (015), (017), (018), (0,1,10), (0,1,11), (110), and (113), which further characterize the LDH phase.[8] It is worth mentioning that all these peaks are much stronger in sample MAO4B than in MAO4A, which was obtained after 5 days of hydrothermal treatment, indicating that long-time aging facilitates the formation of MgAl−OH LDH. The very interesting phenomenon is the formation of a $3R_2$-polytype LDH phase that rarely occurs in the coprecipitation synthesis.[9] In general, this polytype is featured by the diffraction peaks of (014), (017), (0,1,10), etc. and $3R_1$ by peaks of (012), (015), (018), etc.[8] Note that the peaks of this polytype are reduced in relative intensity after longer time treatment (I_{017}/I_{003} in Table 2), suggesting its thermodynamical stability is relatively low.

(12) Iliseev, A. A.; Lukashin, A. V.; Vertegel, A. A.; Tarasov, V. P.; Tret'yakov, Y. D. *Dokl. Chem. (Trans. of Dokl. Akad. Nauk)* **2002**, *387*, 339.
(13) Sato, T.; Fujita, H.; Endo, T.; Shimada, M.; Tsunashima, A. *React. Solids* **1988**, *5*, 219.
(14) Stanimires, T.; Kirov, G. *Appl. Clay Miner.* **2003**, *22*, 295.
(15) Stanimires, T.; Kirov, G.; Dinolova, E. *J. Mater. Sci. Lett.* **2001**, *20*, 453.
(16) McLaughlin, W. J.; White, J. L.; Hem, S. L. *J. Colloid Interface Sci.* **1994**, *165*, 41.
(17) Miyata, S. *Clays Clay Miner.* **1983**, *31*, 305.

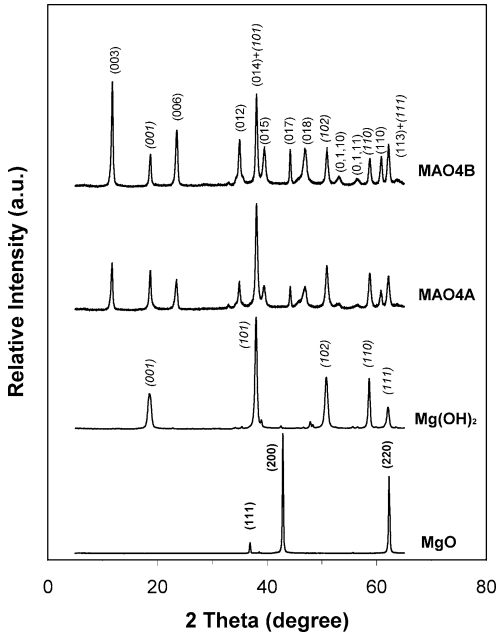

Figure 1. XRD patterns of MAO4A, MAO4B, MgO, and $Mg(OH)_2$. $Mg(OH)_2$ was made from the hydrothermal treatment of MgO in water at 110 °C for 5 days.

Table 2. Phase Composition of As-Prepared Samples Based on XRD Data

	LDH		$Mg(OH)_2$		MgO	
sample	D^a (nm)	$I_{017}/I_{003}{}^b$	D (nm)	$I_{001}/I_{003(LDH)}{}^c$	a (nm)	$I_{200}/I_{003(LDH)}{}^c$
MAO4A	0.756	0.47	0.474	0.76		
MAO4B	0.752	0.33	0.473	0.30		
MACl6	0.787	0.25	0.475	0.48		
MACl4	0.786	0.05	0.473	0.19		
MACl3	0.785	0.07	0.473	0.12		
MACl2	0.787	0.28	0.475	0.07		
MAHC4A	0.754	0.75	0.475	0.07	0.420	1.47
MAHC4B	0.751	0.16	0.474	~0.01	0.420	0.46
MAHC6	0.749	0.03	0.474	0.07	0.420	1.57
MAC4	0.750	~0.01	0.474	0.64	0.420	2.33

[a] The interlayer spacing D of LDH was calculated from those of the (003) and (006) diffraction peaks. [b] The relative intensity of one characteristic diffraction peak (017) of $3R_2$-type LDH was used to indicate its relative amount in the composite. Another peak (014) is overlapped with the (101) peak of $Mg(OH)_2$, not suitable for this purpose. [c] I_{001}, I_{200}, and I_{003} stand for the intensities of peaks (001) of $Mg(OH)_2$, (200) of MgO, and (003) of LDH.

The XRD patterns also show that the impurity phase brucite ($Mg(OH)_2$),[18] indexed in italics in Figure 1, is generated simultaneously and further characterized by the feature vibration at 3697−3698 cm^{-1} (strong and sharp)[19] in the FTIR spectrum of sample MAO4B in Figure 2. As can be seen in Figure 1, however, the initial MgO, well defined in the XRD pattern,[20] completely disappears in the LDH product, being converted into either LDH or brucite.

The infrared absorption peak at 1365 cm^{-1} (CO_3^{2-}, ν_3) and a shoulder at around 3000 cm^{-1} (OH stretching in H-bonded OH···CO_3^{2-}) [3] in the FTIR spectrum of sample MAO4B (Figure 2) show that the LDH phase contains some CO_3^{2-}. However, the morphology of sample MAO4B is much different from that of MgAl−CO_3 LDH (refer to Figure 5). Therefore, the absorption of CO_2 from air occurs during the collection process, and the consequent reaction $CO_2 + OH^- \rightarrow HCO_3^-$ or CO_3^{2-} possibly takes place on the surface of MgAl−OH LDH sheets.

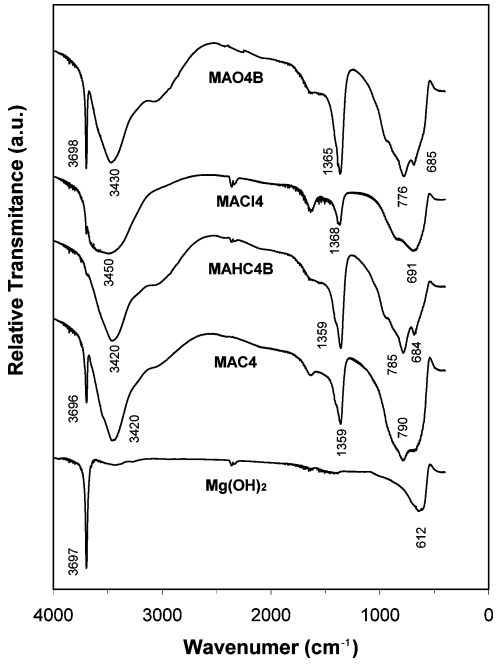

Figure 2. FTIR spectra of MAO4B, MACl4, MAHC4B, MAC4, and $Mg(OH)_2$. $Mg(OH)_2$ was made from the hydrothermal treatment of MgO in water at 110 °C for 5 days.

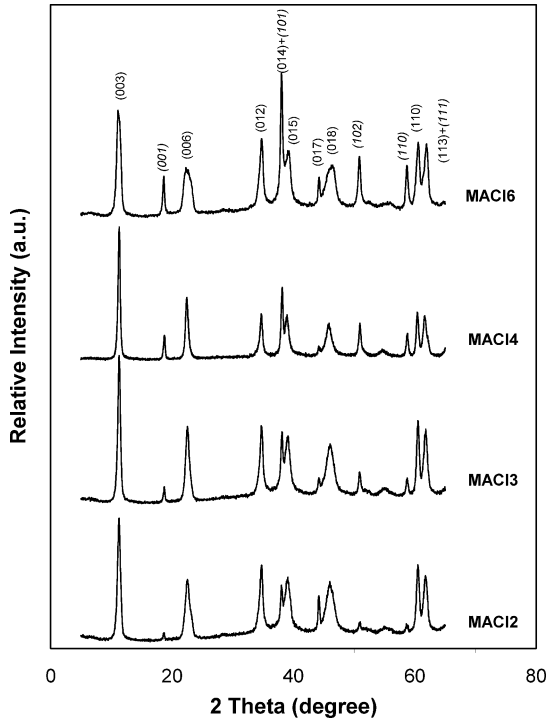

Figure 3. XRD patterns of MACl6, MACl4, MACl3, and MACl2.

Formation of MgAl−Cl LDH. The XRD patterns in Figure 3 show that MgAl−Cl LDH is the dominant phase in these four samples, with the interlayer spacing within 0.785−0.787 nm, as reported elsewhere.[16] Similarly, brucite is formed as a minor component. As the initial ratio of MgO to Al_2O_3 increases from 2 to 6, a bit more brucite phase ($Mg(OH)_2$) is generated, which is clearly indicated by the increase

(18) PCDD Card No. 00-001-1169 for $Mg(OH)_2$.
(19) Bensi, H. A. *J. Chem. Phys.* **1959**, *30*, 852.
(20) PCDD Card No. 00-001-1235 for MgO.

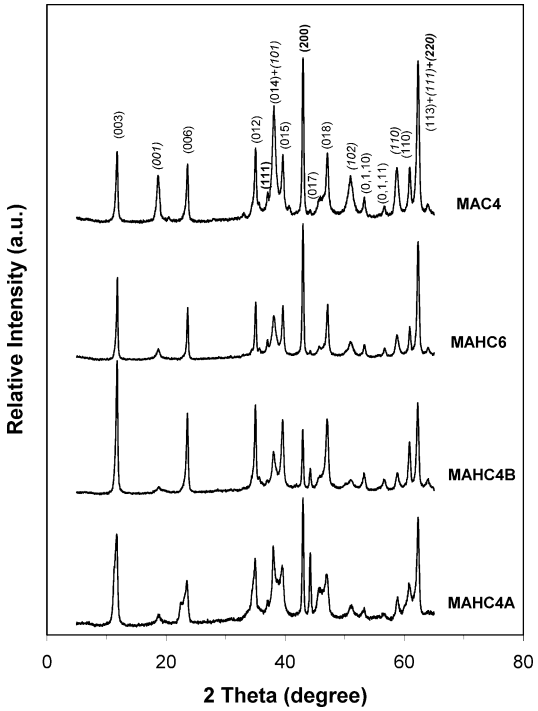

Figure 4. XRD patterns of MAHC4A, MAHC4B, MAHC6, and MAC4.

in the relative intensity $I_{001}/I_{003(LDH)}$ in these samples (Figure 3 and Table 2). $3R_2$-polytype LDH is produced to various extents in these samples. The MgO phase is not observed by XRD either. However, Al_2O_3 (nearly amorphous) in some cases is more than that required for Mg_2Al LDH with the highest charge density in general, and thus believed to exist in some forms in terms of stoichiometry, such as the original Al_2O_3, amorphous AlO(OH), and/or $Al(OH)_3$, although XRD and FTIR cannot identify them.

The typical infrared spectrum of MgAl−Cl LDH is shown in Figure 2 (sample MACl4), with little CO_3^{2-} contamination, as in MgAl−OH LDH.[3] However, the peak at 1365 cm^{-1} (CO_3^{2-}, ν_3) is much weaker. Since the final pH is higher for MgAl−Cl LDH (Table 1), the adsorption of CO_2 from air should be much easier during the collection and much more CO_3^{2-} should be taken up in these samples. The paradox may be that CO_3^{2-} only contaminates the crystallite surface. Since the crystallites in MgAl−Cl LDH are much thicker (Figure 5), there is much less platy surface for the replacement of Cl^- with CO_3^{2-}, and thus less CO_3^{2-} is observed.

Formation of MgAl−CO_3 LDH. The XRD patterns in Figure 4 for MgAl−CO_3 LDHs look different from the previous ones. Although the intensities of diffraction peaks (003), (006), etc. show that the LDH phase is an important component, the diffraction peaks at 43° and 62° are more pronounced.[20] As-formed MgAl−CO_3 LDHs have an interlayer spacing of 0.749−0.754 nm, very close to that of Mg_2Al-CO_3 LDH.[21] Brucite ($Mg(OH)_2$) is only marginally detected by XRD for samples MAHC that were made from a $MgO/Al_2O_3/HCO_3^-$ suspension. However, it is produced in a significant amount in sample MAC4 made from a $MgO/Al_2O_3/CO_3^{2-}$ aqueous mixture (Figures 2 and 4). The intense new diffractions at 43° and 62° in these samples are attributed to the cubic MgO with a unit cell parameter a of 0.420 nm (Table 2), as reported elsewhere.[20]

As also shown in Figure 4, sample MAHC4B (10 days of hydrothermal treatment) has more MgAl−CO_3 LDH and less MgO than sample MAHC4A (5 days of hydrothermal treatment), indicating that the longer aging time facilitates the conversion of MgO and the formation of LDH. We also note in Figure 4 that MAHC4A has stronger (014) and (017) diffraction peaks ($3R_2$-polytype LDH) than MAHC4B, further suggesting the lower thermodynamic stability of the $3R_2$-polytype phase. In addition, samples MAHC6 and MAC4 contain more MgO, but almost no $3R_2$-polytype LDH phase formed.

Morphological Observations. The as-prepared LDHs are quite larger crystallites, with the lateral dimension over 1 μm on average, as can be seen in the SEM images of Figure 5. In particular, the crystallites of MgAl−OH LDH (MAO4B) are very thin but very wide in the lateral dimension (over 5 μm), without a noticeable regular shape observed. For MgAl−Cl LDH and MgAl−CO_3 LDH prepared by 10 days of heat treatment, hexagonally shaped crystallites are formed, with a lateral dimension of 1−3 μm. Such big MgAl−Cl LDH crystallites, in our belief, are reported for the first time. We further believe that this method could be applied to prepare similarly sized LDHs containing other anions. Relatively, MgAl−CO_3 LDH hexagonal sheetlike crystallites are thicker but narrower in the lateral dimension, especially for sample MAC4. It is noted that almost all LDH crystallites are crossed over or interconnected with one another. The elemental analysis by XPS−EDS indicates the existence of Mg and Al and their atomic ratio between 0.14 and 4.12 (Table 1) in these samples.

Discussion

Reaction Pathways. The differences in the crystallite morphology and phase composition are obviously related to the crystallization pathways during the LDH formation. As we know, before and during LDH formation and development some reactions, such as hydrolysis of MgO and Al_2O_3 and dissociation of $Mg(OH)_2$ and $Al(OH)_3$, occur on the surface of the solid particles, simplified as follows:

$$MgO + H_2O \leftrightarrows Mg(OH)_2 \leftrightarrows Mg^{2+} + 2OH^- \quad (1)$$

$$Al_2O_3 + 3H_2O \leftrightarrows 2Al(OH)_3 \leftrightarrows 2Al(OH)_2^+ + 2OH^- \leftrightarrows 2Al(OH)^{2+} + 4OH^- \leftrightarrows 2Al^{3+} + 6OH^- \quad (2)$$

$$Al(OH)_3 + OH^- \leftrightarrows Al(OH)_4^- \quad (3)$$

We suggested that the freshly generated $Mg(OH)_2$ and $Al(OH)_3$, more or less, form thin layers on their own oxide particle surfaces, as shown in the first step in Figure 6, which could prevent the inside oxide phase from being further hydrolyzed. The inside oxide can be further hydrolyzed when the hydroxide layer is dissolved via dissociation. Noticeably, these reactions are all related with hydroxide anion (OH^-) and thus affected by the solution pH. In our experiments, pH is generally increased from ~7 to ~12 (Table 1), which,

(21) PCDD Card No. 01-089-0460 for $Mg_2Al(OH)_6(CO_3)_{0.5}\cdot 1.5H_2O$.

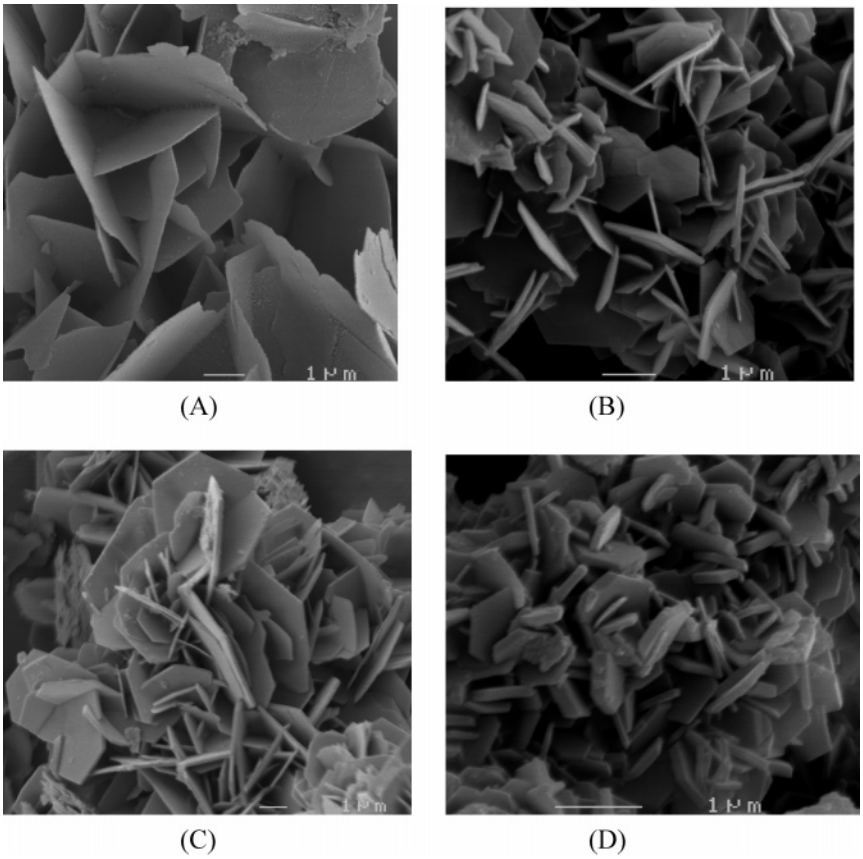

Figure 5. SEM images of (A) MAO4B, (B) MACl2, (C) MAHC4B, and (D) MAC4.

especially the initial pH, plays a very important role in the formation process.

There are several possible Al cationic species as a result of dissociation (Table 3).[22] However, their total concentration is very limited. As shown by the calculation in Table 3, they are very sparse in the suspension at room temperature. For example, at pH 6.5, their total concentration, i.e., $[Al^{3+}] + [Al(OH)_2^{+}] + [Al(OH)^{2+}] + [Al_3(OH)_4^{5+}] + [Al_{13}(OH)_{32}^{7+}]$, is around 10^{-7} M. The higher the pH, the lower their concentration. Therefore, we can ignore their role in the formation of LDH in the later stage when pH $\geq$ 7. Therefore, the possible reactions contributing to the MgAl LDH formation can be envisaged as follows:

$$a\mathrm{Mg(OH)_2(s)} + \mathrm{Al(OH)_3(s)} + x\mathrm{H_2O} + \mathrm{A^-} \leftrightarrows \mathrm{Mg}_a\mathrm{Al(OH)}_{2+2a}\mathrm{A}\cdot x\mathrm{H_2O(s)} + \mathrm{OH^-} \quad (4)$$

$$a\mathrm{Mg^{2+}} + \mathrm{Al(OH)_4^-} + (2a-2)\mathrm{OH^-} + x\mathrm{H_2O} + \mathrm{A^-} \leftrightarrows \mathrm{Mg}_a\mathrm{Al(OH)}_{2+2a}\mathrm{A}\cdot x\mathrm{H_2O(s)} \quad (5)$$

$$a\mathrm{Mg^{2+}} + \mathrm{Al(OH)_3(s)} + (2a-1)\mathrm{OH^-} + x\mathrm{H_2O} + \mathrm{A^-} \leftrightarrows \mathrm{Mg}_a\mathrm{Al(OH)}_{2+2a}\mathrm{A}\cdot x\mathrm{H_2O(s)} \quad (6)$$

$$a\mathrm{Mg(OH)_2(s)} + \mathrm{Al(OH)_4^-} + x\mathrm{H_2O} + \mathrm{A^-} \leftrightarrows \mathrm{Mg}_a\mathrm{Al(OH)}_{2+2a}\mathrm{A}\cdot x\mathrm{H_2O(s)} + 2\mathrm{OH^-} \quad (7)$$

where A^- denotes OH^-, Cl^-, or $^1/_2CO_3^{2-}$. Since the direct

(22) Öhman, L.-O. *Inorg. Chem.* **1988**, *27*, 2565.

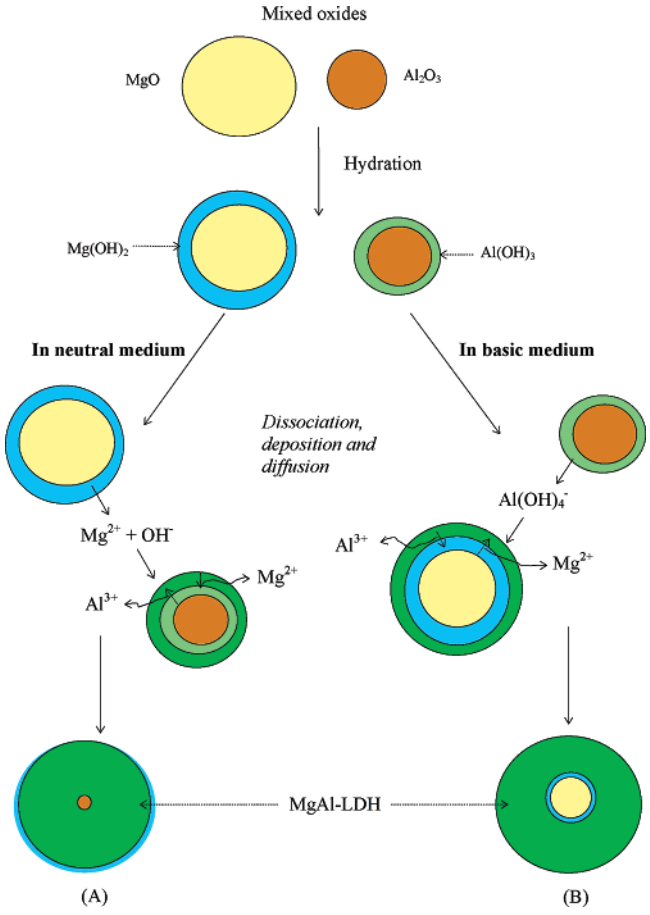

Figure 6. Suggested scheme for LDH formation from mixed MgO and Al_2O_3 in a (A) neutral and (B) basic aqueous solution.

Table 3. Calculated Concentrations of Some Metal Ion Species

equilibrium reaction	pK_{sp} at 25 °C	metal ion species	metal ionic species concentration (M)				
			pH 6.5	pH 7.0	pH 8.3	pH 10.0	pH 11.5
$Mg(OH)_2(s) \leftrightarrows Mg^{2+} + 2OH^-$	10.0[a]	Mg^{2+}	1.0×10^{5}	1.0×10^{4}	2.5×10^{1}	1.0×10^{-2}	1.0×10^{-5}
$Al(OH)_3(s) \leftrightarrows Al^{3+} + 3OH^-$	31.2[a]	Al^{3+}	2.0×10^{-9}	$6.3\ 10^{-11}$	7.9×10^{-15}	6.3×10^{-20}	0[c]
$Al(OH)_3(s) \leftrightarrows Al(OH)_2^+ + OH^-$	14.5[b]	$Al(OH)_2^+$	1.0×10^{-7}	3.2×10^{-8}	1.6×10^{-9}	3.2×10^{-11}	1.0×10^{-12}
$Al(OH)_3(s) \leftrightarrows Al(OH)^{2+} + 2OH^-$	22.7[b]	$Al(OH)^{2+}$	2.0×10^{-8}	2.0×10^{-9}	5.0×10^{-12}	2.0×10^{-15}	2.0×10^{-18}
$3Al(OH)_3(s) \leftrightarrows Al_3(OH)_4^{5+} + 5O\ H^-$	51.2[b]	$Al_3(OH)_4^{5+}$	2.0×10^{-14}	6.3×10^{-17}	0	0	0
$13Al(OH)_3(s) \leftrightarrows Al_{13}(OH)_{32}^{7+} + 7O\ H^-$	66.8[b]	$Al_{13}(OH)_{32}^{7+}$	5.0×10^{-15}	1.6×10^{-18}	0	0	0
$Al(OH)_3(s) + OH^- \leftrightarrows Al(OH)_4^-$	1.3[b]	$Al(OH)_4^-$	6.3×10^{-7}	2.0×10^{-6}	4.0×10^{-5}	2.0×10^{-3}	6.3×10^{-2}

[a] K_{sp} data of fresh $Mg(OH)_2$ and $Al(OH)_3$ were from ref 10. [b] The original hydration constants of Al^{3+} were from ref 22, but the equilibrium constants here were derived from these data. [c] Zero means the concentration is less than 1×10^{-20} M.

contact between the freshly formed $Mg(OH)_2$ and $Al(OH)_3$ is very limited, the contribution of eq 4 can be neglected.

On the other hand, $Al(OH)_4^-$ is the predominant Al species in the solution. In general, its concentration increases proportionally to $[OH^-]$. For example, its concentration is 2.0×10^{-6} M at pH 7, 4.0×10^{-5} M at pH 8.3, and 2.0×10^{-3} M at pH 10.0. In practice, $[Mg^{2+}]$ is possibly 10^{-3}–10^{-4} M since the solubility of fresh $Mg(OH)_2$ is 2.9×10^{-4} M theoretically albeit the calculated Mg^{2+} equilibrium concentration at pH $\leq$ 10 is much higher (Table 3). Therefore, the ionic precipitation in eq 5 may occur to some degree, but limited. We believe that eqs 6 and 7 determine the direction of the formation of different LDHs and other components, as addressed in later sections.

LDH Formation under Neutral and Basic Conditions. In the neutral solution, we believe that the deposition of Mg^{2+} and OH^- onto the surface of $Al(OH)_3/Al_2O_3$ particles (Figure 6A and eq 6) directs the hydrothermal formation of LDHs. At pH 7.0 or 6.5, $Al(OH)_4^-$ is relatively rare, around $10^{-6.0}$ M (Table 3). As proposed in Figure 6A, the dissociation of $Mg(OH)_2$ into Mg^{2+} and OH^- is possibly the key event. As a consequence, such a deposition helps to form the MgAl pre-LDH phase. As more Mg^{2+} and OH^- deposit and more Mg^{2+} and Al^{3+} ions diffuse in the lattice upon heat treatment at 110 °C (Figure 6A), more and well-defined MgAl LDH is finally formed.

In contrast, in a basic medium, such as in HCO_3^- or CO_3^{2-} solution, pH is higher; thus, $Al(OH)_4^-$ could reach up to 4.0×10^{-5} M (pH 8.3), and more importantly, the dissociation of $Mg(OH)_2$ is somewhat inhibited. Therefore, as shown in Figure 6B and eq 7, the deposition of $Al(OH)_4^-$ into the $Mg(OH)_2$ lattice to form MgAl pre-LDH is favored. The simultaneous bilateral diffusion homogenizes the cation distribution to give rise to a well-defined LDH phase. In this case, some unhydrated MgO is buried underneath the freshly formed MgAl LDH and is observed by XRD.

A Generalized LDH Formation Mechanism and Its Validity. On the basis of the above discussion and more systematic experimental results, we propose a dissociation–deposition–diffusion mechanism via two possible pathways for the LDH formation as a general model for all LDH preparations, as represented in Figure 6. First, because the bilateral diffusion of cations in both pathways is a slow process, a longer time in hydrothermal (or aging in general) treatment will facilitate such diffusion and produce more thermodynamically stable LDH. This is what we observed for samples MAO4A/MAO4B and MAHC4A/MAHC4B. Second, more and more $Mg(OH)_2$ molecules are observed

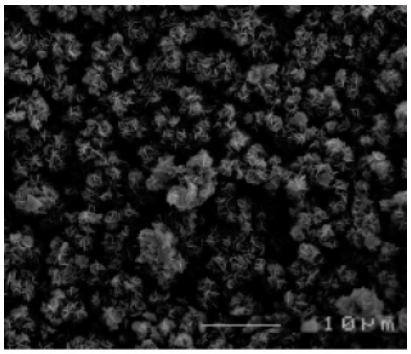

(A)

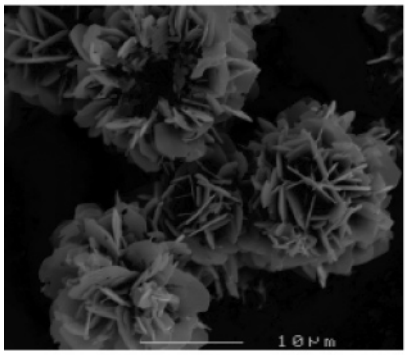

(B)

Figure 7. SEM images of (A) MACl2 and (B) MAHC6 on a 10 μm scale.

for samples MACl2 to MACl6 as the ratio of MgO to Al_2O_3 increased from 2 to 6. Since the surface area of $Al(OH)_3/Al_2O_3$ and the diffusion of Al^{3+} in the lattice (Figure 6A) should be similar in these cases, the resultant LDH should be similar and thus more $Mg(OH)_2$ is formed owing to the higher initial MgO content and higher pH (Table 1). Third, the MgO phase is observed only in the basic medium (Figure 4). This can only occur when MgO is wrapped inside the LDH phase. Otherwise, MgO will no longer exist in water, but will be transformed into $Mg(OH)_2$. As a matter of fact, sample $Mg(OH)_2$ as examined by XRD in Figure 1 and FTIR in Figure 2 was hydrothermally formed from MgO in pure water.

The morphological features of the samples in Figure 7 seem to support the above mechanism. The aggregates, like sand roses,[16] are LDH sheets grown on the surface of MgO or Al_2O_3. It is seen that the particles in sample MAHC6 ($\sim$20 μm) are about 10 times bigger than those in sample MACl2 ($\sim$2 μm). As we know, Al_2O_3 has a surface area (121 m^2/g) 14 times as large as that of MgO (8.3 m^2/g), and therefore, Al_2O_3 particles (seeds) would be 14 times smaller. In this regard, the growth of LDH on the Al_2O_3 seeds will lead to

relatively smaller aggregates as in the case of MACl2 (Figure 7A) while LDH aggregates growing on the MgO seed will be much bigger as in the case of MAHC6 (Figure 7B).

The surface elemental analysis from XPS−EDS data can also support the general LDH growth mechanism. For example, the [Mg]/[Al] atomic ratio in sample MACl6 is 1.789, much higher than that in sample MAHC6 (1.078), suggesting more Mg^{2+} on the surface in sample MACl6 than in sample MAHC6. In the very extreme case of MAC4, whose initial solution is very basic (pH 11.5), only a small amount of Mg ([Mg]/[Al] = 0.140) is detected. In such a strong basic solution (pH 11.5), $Al(OH)_4^-$ will be very high, possibly up to 0.06 M theoretically, while the dissociation of $Mg(OH)_2$ is severely prohibited and Mg^{2+} ($10^{-5.0}$ M) can be neglected (Table 3). Therefore, the deposition of $Al(OH)_4^-$ onto the $Mg(OH)_2$/MgO surface to form pre-LDH will be very much preferred, thus further blocking the dissociation of $Mg(OH)_2$ and encapsulating MgO inside. This would be the reason more MgO is observed by XRD (Figure 4, MAC4) while very little Mg on the surface is detected by XPS−EDS (Table 1, MAC4). However, similar [Mg]/[Al] atomic ratios in samples MAHC4B (1.383) and MACl4 (1.225) would not say so. We believe that the initial pH is not the only determining factor. As the dissociation of $Mg(OH)_2$ and the deposition of Mg^{2+}/OH^- on $Al(OH)_3/Al_2O_3$ occur (Figure 6A), the pH increases in sample MACl4 (the final pH is 11.9). The increase in pH causes the uncovered $Al(OH)_3$ to be ionized into $Al(OH)_4^-$, and therefore, the reserve deposition of $Al(OH)_4^-$ on $Mg(OH)_2$/MgO could take place. On the other hand, sample MAHC4B has a pH range of 8.3−9.7, and the deposition of $Al(OH)_4^-$ onto $Mg(OH)_2$/MgO proceeds while uncovered $Mg(OH)_2$ may be simultaneously dissociated. The released Mg^{2+} ions would deposit on the surface of $Al(OH)_3/Al_2O_3$ to form the other type of pre-LDH phase. Therefore, the later joined pathways flatten the difference in the composition.

In summary, the dissociation−deposition−diffusion mechanism via two different pathways shown in Figure 6 is the likely mechanism that directs the formation and growth of MgAl LDH from mixed MgO and Al_2O_3 oxides in two extreme cases, particularly in the initial stage. It is noted that these two pathways take place simultaneously to contribute to the formation of LDH as the pH is in the range of 8−10. Once the possible species, i.e., $Mg(OH)_2$ or $Al(OH)_3$, is all converted into less soluble MgAl LDH, the so-called dissolution−recrystallization process may start to form big crystallites.[14] Since the dissolution and recrystallization, or more precisely, dissociation and deposition, of Mg and Al species occur at different rates, we believe that the process is a combination of these two pathways with an overall slow rate.

Implication of the General LDH Formation Mechanism. The coprecipitation method for LDH preparation is actually not a coordinated process leading to the uniform LDH phase. In a real titration of Al^{3+} and Mg^{2+} chloride with sodium hydroxide solution, as reported by Braterman et al., the precipitation is a two-step process.[10,11] The first step at a pH of ∼4 is associated with the formation of $Al(OH)_3$, while the second one at a pH of ∼8 is attributed to the $Mg^{2+} + OH^-$ precipitation onto the $Al(OH)_3$ surface to form the pre-LDH hydroxide mixture. The material obtained at this stage is initially in the form of aggregates with very poor crystallinity, but becomes well crystallized when it is subject to several hours of aging. Such phenomena are consistent with our LDH formation mechanism (Figure 6A). The second precipitation, e.g., the deposition of $Mg^{2+} + OH^-$ onto $Al(OH)_3$, is somewhat like the deposition in route A of Figure 6. The heat treatment then facilitates the bilateral diffusion of Al^{3+} and Mg^{2+} in the solid lattice and homogenizes the distribution of Mg^{2+} and Al^{3+} to form uniform LDH.[23] It is worth noting that $Mg^{2+} + OH^-$ deposit on $Al(OH)_3$ at much lower pH (7−8) than pure Mg^{2+} does (pH 9−9.5),[3] which suggests that the pre-LDH hydroxide mixture is much less soluble than $Mg(OH)_2$. This seems to support the point in our hypothesis that once the pre-LDH phase is formed on the surface of $Mg(OH)_2$/MgO or $Al(OH)_3/Al_2O$ particles, it prevents the inside materials from further changing. Apparently, the so-called homogeneous preparation of MgAl LDH is very similar to this. Slowly hydrolyzing urea in water causes the pH to increase, and thus, Al^{3+} ions first precipitate at a pH of ∼4.0, followed by the deposition of Mg^{2+} and OH^- on the surface of $Al(OH)_3$ when the pH increases to 7−8[1,4] and the conversion to the well-crystallized LDH phase. Such a process could also occur in nature. The bayerite ($Al(OH)_3$) or boehmite (AlO(OH)) in nature may take up the free Mg^{2+}, OH^-, and HCO_3^-/CO_3^{2-} in natural water to form less soluble pre-LDH material as well as well-defined LDH even at pH 6−7 through the processes represented in Figure 6. In addition, the constant pH preparation of MgAl LDH is another example since more insoluble $Al(OH)_3$ may quickly precipitate and then Mg^{2+}/OH^- deposits to lead to a similar pre-LDH material.

Reconstruction from mixed oxide is the other way to prepare LDH. Mixed oxide, e.g., MgAl oxide, is generally obtained by calcining the corresponding LDH at a mild temperature (400−600 °C). The decomposition process of solid LDH is suggested to occur topotactically,[24] and thus the cations are evenly distributed in the mixed oxide. In this connection and on the basis of SEM observations, Sato et al.[13] proposed that the reconstruction of LDH from such an oxide in Na_2CO_3 solution proceeded topotactically. Obviously, the topotactic process is only one possible process. If it is the only process, the LDH first formed on the surface of mixed oxide particles will prevent the proceeding of the inside oxide to LDH, and thus, the MgO phase (NaCl-type oxide), more or less, should be observed in XRD. However, this has not been reported elsewhere.[6] It should be mentioned that the formation of LDH from physically mixed MgO and Al_2O_3 in our experiments does not support such a mechanism.[13] In addition, the bigger crystallites formed from reconstruction cannot be explained by the topotactic process, but by our generalized formation mechanism.

As reported by McLaughlin et al.,[16] LDH formation occurs upon mixing magnesium hydroxide and aluminum hydroxy-

(23) Reichle, W. T. *Solid States Ionics* **1986**, *22*, 135.
(24) Markov, L.; Petrov, K.; Lynbchova, A. *Solid State Ionics* **1990**, *39*, 187.

carbonate suspensions. They have found that the higher the initial pH in the mixed suspension, the sooner the LDH forms. They proposed that the nucleation and growth of LDH occurs directly on the magnesium hydroxide surface, which is in agreement with the proposed mechanism in Figure 6B by using $Al(OH)_4^-$ as the intermediate carrier at a relatively high pH. In Sato's case where the pH is around 11, we believe that the mechanism in Figure 6B dominates the reconstruction process. On the other hand, Jones et al.[9] reconstructed LDH directly from mixed MgO and Al_2O_3 oxides with the initial pH close to 7. As we suggested, the mechanism in Figure 6A dominates the initial process while route B (Figure 6B) comes on in tandem as the pH increases to, for example, 9−10 in our experiments.

Relationship between Intercalated Anions and Morphologies. The difference in morphology is closely related to the concentration of the counteranions available. In the cases presented in this work, $[Cl^-]$ and $[HCO_3^-]$ are around 0.10 M and $[CO_3^{2-}]$ is no less than 6.0×10^{-4} M while $[OH^-]$ is from 1×10^{-7} M at the beginning to 1×10^{-4} M at the end for samples MAO4A and MAO4B. Therefore, once the positively charged hydroxide layers are formed, the abundant Cl^-, HCO_3^-, or CO_3^{2-} ions are quickly adsorbed on the surface of these layers. The adsorbed anion layer becomes a platform for the next layer generation, thus leading to thicker crystallites.[25] In contrast, the sparse OH^- in the solution can hardly form such an anion layer, and even worse, the OH^- ions prefer combining with metal ions to form the hydroxide layers to being loosely adsorbed on the hydroxide layers. Therefore, the growth along the lateral dimension is preferred, producing very thin but very wide MgAl−OH LDH sheets (Figure 5). In addition, some of the interconnections between the LDH crystallites (Figures 5 and 7) may arise from the sharing of the oxide seed but growing along different directions.

(25) Xu, Z. P.; Braterman, P. S. *J. Mater. Chem.* **2003**, *13*, 268.

Conclusions

Layered double hydroxides formed from physically mixed MgO and Al_2O_3 oxides in aqueous suspension upon hydrothermal treatment for 5 and 10 days are systematically studied. The formation is strongly affected by the initial pH of the suspension. Under the initially neutral conditions, MgAl LDH is formed with $Mg(OH)_2$ as a minor impurity. In the basic conditions, however, LDH is also generated, but the major impurity is MgO that is not hydrated even after 10 days of heating. As-prepared LDHs, except for MgAl−OH LDH, exhibit a well-developed hexagonal plate sheet with a lateral dimension of over 1 μm, typical for homogeneously precipitated MgAl−CO_3 LDH. Therefore, this hydrothermal method can be used to prepare big LDH crystallites.

On the basis of the experimental observations on the LDH formation, we propose a general dissociation−deposition−diffusion mechanism that includes two possible pathways to explain the LDH formation and growth. In the nearly neutral condition, $Mg(OH)_2$ from MgO hydration is dissociated to Mg^{2+} and OH^-, which deposit on the surface of $Al(OH)_3/Al_2O_3$ to form the pre-LDH phase. In the basic solution, ionization of $Al(OH)_3$ gives rise to abundant $Al(OH)_4^-$ ions which deposit on the surface of $Mg(OH)_2$ to form pre-LDH hydroxide. Continuous heating facilitates the bilateral diffusion of metal ions in the lattice and thus leads to the formation of uniform and well-crystallized LDHs.

Acknowledgment. This work is produced as part of the activities of the ARC Centre for Functional Nanomaterials funded by the Australia Research Council under its Centre of Excellence Scheme.

CM048085G